

## Resonance Shifting by Ferrite Thick Film Superstrate

Maruti Rendale<sup>1</sup>, Shrihar Mathad<sup>2</sup>, Vijaya Puri<sup>3</sup>

**Abstract:** Fritless thick films of Ni-Co-Zn ferrites were fabricated by screen printing technique on alumina substrates. Structural analysis was undertaken using X-ray diffraction and Scanning electron microscopy techniques. A new approach for the determination of complex permittivity ( $\epsilon'$  and  $\epsilon''$ ) using microwave property perturbation is unveiled. Ag thick film microstrip ring resonator (MSRR) with and without the thick film substrate was used for the microwave transmission studies in the frequency region of 8–12 GHz. The microwave conductivity of the thick films lies in the range of 1.779 S/cm to 2.296 S/cm. The penetration depth is also reported within the X-band of microwave frequencies.

**Keywords:** Thick films, Microstrip ring resonator (MSRR), Complex permittivity, Penetration depth.

### 1 Introduction

Ferrites symbolize a significant category of materials, which are predominantly employed, due to their numerous practical applications, such as magnetic devices in electronic, optical and microwave installations [1]. [Spinel ferrites, with common formula of  $MFe_2O_4$  (M is various divalent or trivalent metals cations) have been extensively used in various components for applications in the high-frequency range due to their high electrical resistivity, high permeability, and chemical stability. Substituted Ni-Zn ferrites have a wide range of applications in radio frequency (RF) electronic devices due to the high initial permeability in combination with high resistivity [2]. Ni-Zn ferrites with their ease of preparation and versatility for use in wide ranging application are very attractive materials from the commercial point of view. Ni-Zn ferrites with high permeability and high frequency are widely used in the telecommunications, electronics and information technology, surface-mount technology and various sensors. Properties of ferrites dependent upon several factors such as composition, method of preparation, doping of different cations, sintering

---

<sup>1</sup>Department of Physics, KLS Gogte Institute of Technology, Belagavi, India; E-mail: [physicssiddu@gmail.com](mailto:physicssiddu@gmail.com)

<sup>2</sup>K.L.E. Institute of Technology, Hubli, India; E-mail: [physicssiddu@kleit.ac.in](mailto:physicssiddu@kleit.ac.in)

<sup>3</sup>Department of Physics, Shivaji University, Kolhapur, India; E-mail: [vijayapuri@gmail.com](mailto:vijayapuri@gmail.com)

temperature and time, sintered density, grain size and their distribution [2 – 3]. Ferrite properties are highly dependent on the methodology espoused for their synthesis, preparative conditions, sintering temperature (time), chemical composition, and grain size etc. [4].

Ni-Zn ferrites have a mixed spinel ferrite structure and are used as a wave absorber for electromagnetic interference [5]. Spinel type ferrites are commonly used in many electronic and magnetic devices due to their high magnetic permeability and low magnetic losses [6, 7] and also used in electrode materials for high temperature applications because of their high thermodynamic stability, electrical resistivity and electrolytic activity [8]. Moreover, these low cost materials are easy to synthesize and offer the advantages of greater shape formability than their metal and amorphous magnetic counterparts. Almost every item of electronic equipment produced today contains some ferrimagnetic spinel ferrite materials. Loudspeakers, motors, deflection yokes, electromagnetic interference suppressors, radar absorbers, antenna rods, proximity sensors, humidity sensors, memory devices, recording heads, broadband transformers, filters, inductors, etc. are fabricated with ferromagnetic (ferrite) material as a major component.

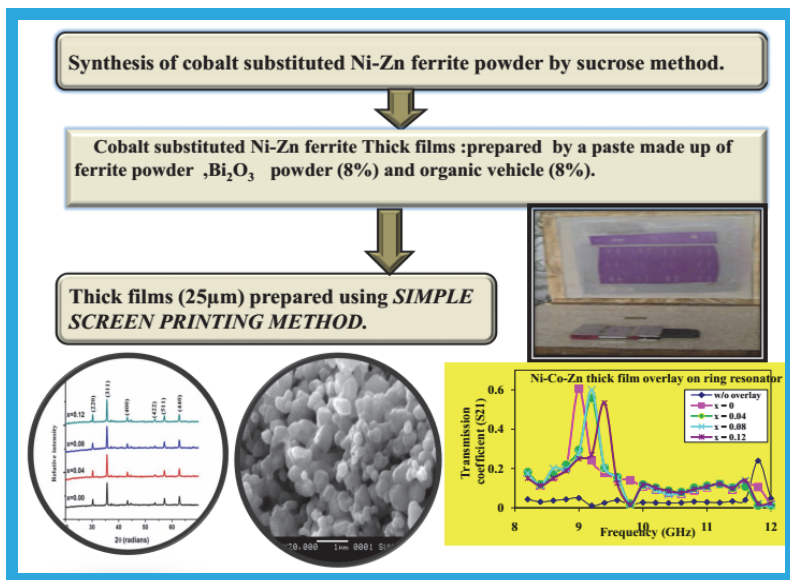


Fig. 1 – Schematic flow-chart of work.

This paper reports the fabrication of Ni<sub>0.7-x</sub>Co<sub>x</sub>Zn<sub>0.3</sub>Fe<sub>2</sub>O<sub>4</sub> thick films by cost effective and accurate technique of screen printing. The numerous parameters such as crystallite size, d-spacing, lattice constant, strain, dislocation density and packing fraction of un-doped and cobalt doped Nickel-Zinc ferrite

calculated by X-ray diffraction patterns are presented. The complex permittivity, microwave conductivity and penetration depth are also evaluated by microstrip ring resonator property perturbations

## 2 Result and Discussions

### 2.1 Materials and methods

The nanoferrite  $\text{Ni}_{0.7-x}\text{Co}_x\text{Zn}_{0.3}\text{Fe}_2\text{O}_4$  ( $x = 0, 0.04, 0.08$  and  $0.12$ ) thick films were fabricated by screen printing technique. The ferrite powder samples were mixed with 7% of  $\text{Bi}_2\text{O}_3$  by weight in an agate mortar and pestle and the organic vehicle (prepared by dissolving ethyl cellulose in to [2-(2-Butoxy ethoxy)-ethyl]-acetate was added drop wise till a viscous paste sufficient for screen printing was formed. Films do not containing, glass as one of the constituents in the adhesive substance known as Fritless films. Then the thick films were delineated on alumina substrates of size (2 cm x 1 cm) by screen printing technique. The films were dried under IR lamp for 12 hours and then fired at  $900^\circ\text{C}$ . Thickness of the films was maintained to be about  $30\mu\text{m}$ . The thick films were subjected to X-ray diffraction on a PHILIPS diffractometer (Model-1710) with  $\text{Cu-K}\alpha$  radiation at a wavelength of  $\lambda = 1.542\text{\AA}$ . The surface morphology of the films were observed with a scanning electron microscope (JEOL-JSM- 6360). The ferrite thick films were kept as superstrate on the Ag-thick film microstrip ring resonator (resonant frequency 11.7 GHz) and microwave transmittance was measured.

### 2.2 Structural studies

The XRD patterns [PHILIPS DIFFRACTOMETER MODEL-1710,  $\text{Cu-K}\alpha$ -radiations of  $\lambda = 1.542 \text{\AA}$ ] shown in Fig. 2 confirmed the formation of cubic ferrite phase in all the samples. The main reflection planes of the cubic structure of the ferrite crystals are (220), (331), (400), (420), (551) and (440). The lattice parameter, cell volume and crystallite size of the thick films are tabulated in Table1. It is evident that, as cobalt concentration increases the lattice parameter increases in accordance with the Vegard's law. Fig. 2 shows the X-ray diffraction patterns of  $\text{Ni}_{0.7-x}\text{Co}_x\text{Zn}_{0.3}\text{Fe}_2\text{O}_4$  ( $x=0.00, 0.04, 0.08$  and  $0.12$ ) thick films.

The interplanar spacing  $d$  was calculated using the formula,

$$d = \frac{a}{(h^2 + k^2 + l^2)^{1/2}} \quad (1)$$

Crystallite size is a measure of the size of a coherently diffracting domain. The average grain size was estimated by measuring the peak width at half length of full maxima for the different compositions by using Debye –Scherer's formula [11]

$$D = \frac{0.9\lambda}{\beta \cos \theta}, \quad (2)$$

where  $\beta$  full width half maxima,  $\lambda$  wavelength of the X-ray.

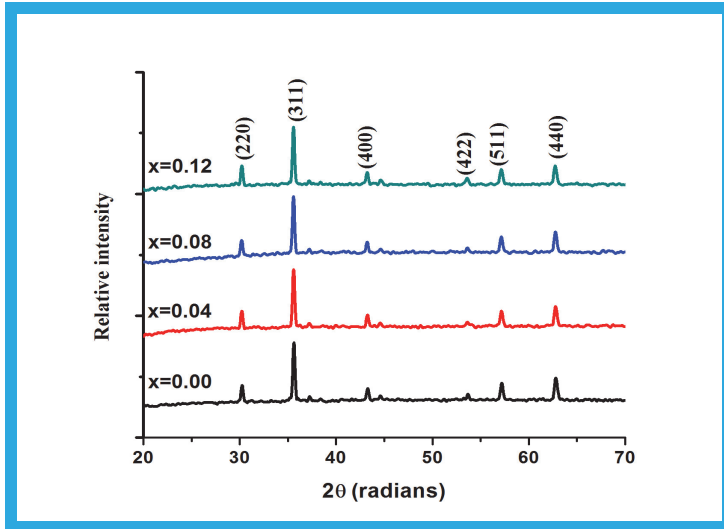


Fig. 2 – XRD patterns of Ni-Co-Zn Ferrite.

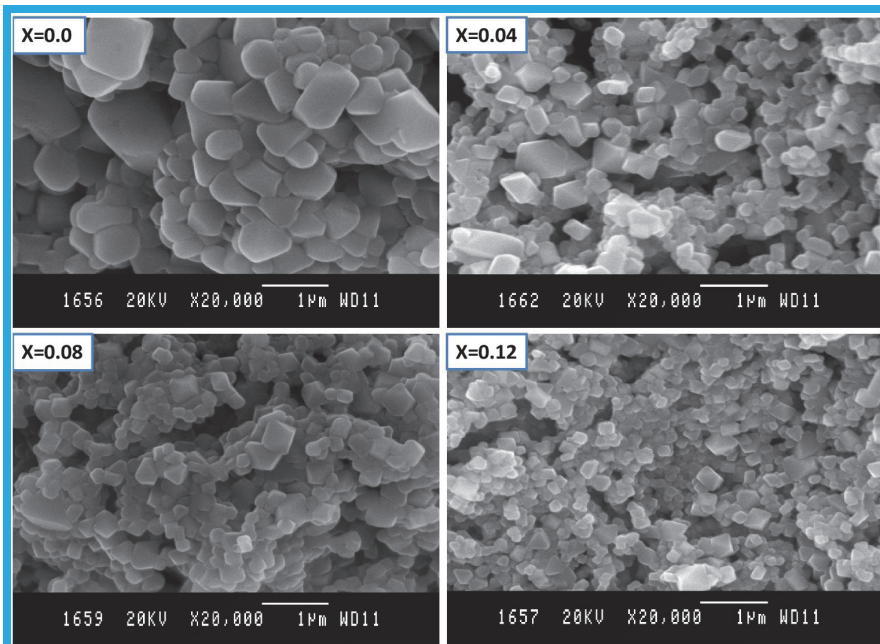
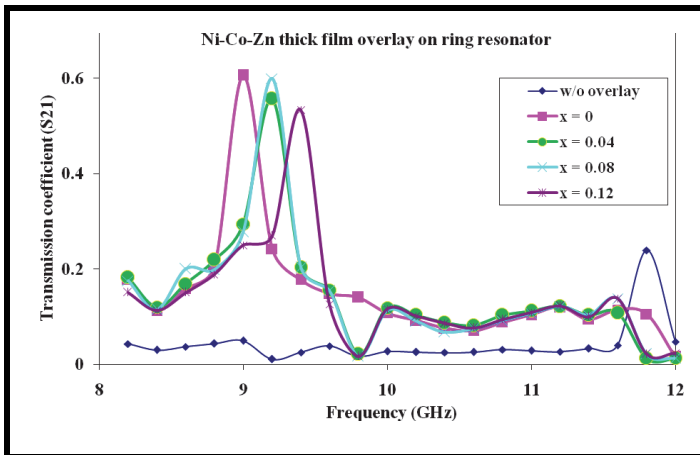


Fig. 3 – SEM Images Ni-Co-Zn Ferrite.

The average crystallite size lies in the range of 69–119nm and is found to increase with the increase in cobalt concentration. Generally, crystallite size will not be the same throughout the crystal, as the presence of polycrystallinity causes aggregation. It is found that the lattice parameter changes with the change in cobalt content. On the basis of ionic radii the change of the lattice parameter is explained as follows: radius of the  $\text{Co}^{2+}$  ion (0.745 Å) is greater than that of the  $\text{Ni}^{2+}$  ion (0.69 Å). The nickel ions with smaller ionic radii are partially replaced by the cobalt ions and leads to the enlargement of the unit cell dimensions, resulting in the increase in lattice parameter.

Fig. 3 depicts the SEM images of thick films of  $\text{Ni}_{0.7-x}\text{Co}_x\text{Zn}_{0.3}\text{Fe}_2\text{O}_4$ . The morphology of the samples indicates that the thick film with  $x = 0$ , consists of non uniform cubic grains separated by grain boundaries and larger voids showing higher porosity. However almost uniform size cubes are seen in the micrographs of the other samples, which contain cobalt ( $\text{Co}^{+2}$ ). The absence of segregation of impurity phases or oxides in the grain boundaries is evidenced in all the thick films. The voids seen in the sample with  $x = 0$  are found to disappear in the samples with the higher concentration of  $\text{Co}^{2+}$ . The number and size of voids are found to decrease with the increase in cobalt concentration, exhibiting the material of  $\text{Ni}_{0.7-x}\text{Co}_x\text{Zn}_{0.3}\text{Fe}_2\text{O}_4$  becoming more nano-crystalline due to the substitution of cobalt.



**Fig. 4** – Response of Ag thick film MSRR due to Ni-Co-Zn Ferrite (Thick films).

This results in to a decrease in porosity or increase in physical density of the material. The close packing of the grains is found to be favored by the concentration of  $\text{Co}^{2+}$  ions, suggesting the densification of the  $\text{Ni}_{0.7-x}\text{Co}_x\text{Zn}_{0.3}\text{Fe}_2\text{O}_4$  ferrites material. The average grain size was evaluated using SEM micrographs by intercept method. The average grain size for the samples

with  $x = 0, 0.04, 0.08$  and  $0.12$  is  $0.372 \mu\text{m}, 0.268 \mu\text{m}, 0.243 \mu\text{m}$  and  $0.208 \mu\text{m}$  respectively. The grain size of Ni-Co-Zn ferrite system, decreases with the increase in cobalt concentration ( $x$ ). Generally, smaller grains imply larger number of insulating grain boundaries, which lead to increase in the porosity of a ferrite material. It is evident from the X-ray diffraction studies that, in the present case, porosity decreases with the increase in  $\text{Co}^{2+}$  concentration, which is an anomalous result that the decrease in grain size is leading to decrease in porosity or increase in physical density of the ferrite material. In other words, even though the grain boundaries are large in number due to the decrease in grain size, the voids are lesser in the samples with higher concentration of cobalt. Hence it can be concluded that the increase in  $\text{Co}^{2+}$  concentration in the Ni-Co-Zn ferrites lead to densify the material [10].

### **2.3 Microwave dielectric studies by overlay method**

Superstrate method means a thick film overlaid on the microstrip ring resonator. For superstrate studies, thick films of  $\text{Ni}_{0.7-x}\text{Co}_x\text{Zn}_{0.3}\text{Fe}_2\text{O}_4$  ferrites were kept in touch on the microstrip ring resonator (MSRR) covering the coupling gaps and the transmittance measurements were carried out. The variations of transmission coefficient ( $S_{21}$ ) as a function of frequency for the microstrip ring resonator without and with thick film superstrate is presented in the Fig. 4. Without superstrate (WS) the resonance was observed at 11.7 GHz with a highest transmittance of 23.93%. The substantial increase in transmission coefficient is observed due to the thick film substrates. It is also observed that, resonance peaks shift towards a shorter frequency due to the superstrates of the thick films. The resonant frequency decreases with the decrease in cobalt content.

These variations are due to the change in even mode characteristic impedance as the consequence of perturbations due to the superstrate. The peak shifting towards a shorter frequency has been reported to be due to even mode coupling, in which contribution of transmission is also prominent [11, 12]. When the resonator is covered with the superstrate of  $\text{Ni}_{0.7-x}\text{Co}_x\text{Zn}_{0.3}\text{Fe}_2\text{O}_4$  thick films of compositions  $x = 0, 0.04, 0.08$  and  $0.12$ , the new resonance frequencies obtained are 9GHz, 9.1GHz, 9.2GHz and 9.4GHz with the resonant transmittance of 60.62%, 59.93%, 55.62% and 53.36 % respectively. The resonance transmittance was found to decrease with the increase in cobalt concentration of the overlay material. The dielectric superstrate perturbs the fringing field of the microstrip component. The  $\text{TM}_{11}$  is the dominant mode for the microstrip ring resonator.

The complex permittivities of  $\text{Ni}_{0.7-x}\text{Co}_x\text{Zn}_{0.3}\text{Fe}_2\text{O}_4$  thick films were calculated from the frequency shift of the microstrip ring resonator due to ferrite superstrate using the formulae [12]

$$\epsilon' = 1 + \frac{C_0}{K} \left\{ \left( \frac{f_a}{f_r} \right)^2 - 1 \right\} \quad \text{and} \quad \epsilon'' = \frac{N'}{f_r r_0}, \quad (3)$$

where the ratio  $\frac{C_0}{K}$  is a constant term related to the standard alumina sample (substrate) given by,

$$\frac{C_0}{K} = \frac{\epsilon'_s - 1}{\left( \frac{f_a}{f_s} \right)^2 - 1}, \quad (4)$$

$\epsilon'_s$  is the permittivity of the standard sample,  $f_r$ ,  $f_a$  and  $f_s$  are the resonant frequencies without superstrate, with superstrate of ferrite samples and standard alumina samples respectively.

$$N' = \epsilon'_s f_s r_{0s}. \quad (5)$$

Here  $r_{0s}$  is the reflection coefficient of ferrite samples and standard sample respectively. The dielectric constant and loss factor lie in the range of 14-17.85 and 3.86-6.27 respectively and both are found to decrease with cobalt (x) content of the ferrite films.

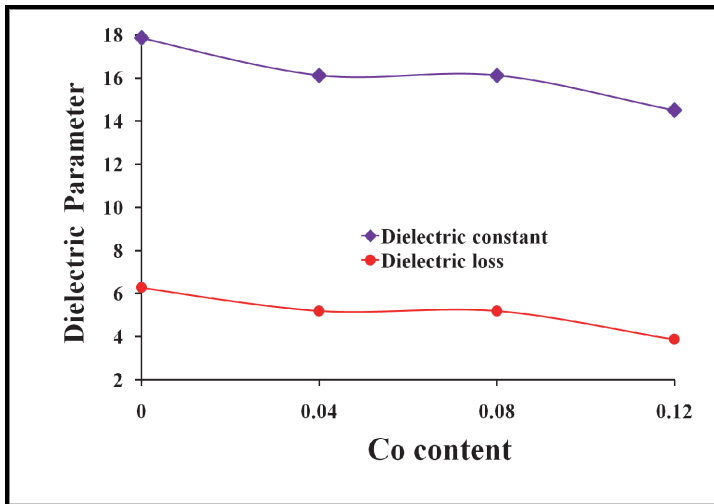


Fig. 5 – Variation of dielectric constant and dielectric loss of thick film as Co content.

The penetration depth of microwave in the ceramics can be calculated by using the following relation [13]

$$D = \frac{c}{\omega} \left\{ 2 \epsilon' \left( 1 + \left( \frac{\epsilon''}{\epsilon'} \right)^2 \right)^{1/2} - 1 \right\}^{-1/2}, \quad (6)$$

where  $c$  is speed of light,  $\omega$  is angular frequency,  $\epsilon'$  and  $\epsilon''$  permittivity of free space and dielectric loss of the material respectively. The variation of penetration depth (reciprocal of attenuation coefficient) with the cobalt composition of thick films is presented in the Fig. 6. The penetration depth ranges from  $27.35 \times 10^{-3}$  -  $32.20 \times 10^{-3}$  m for the thick films.

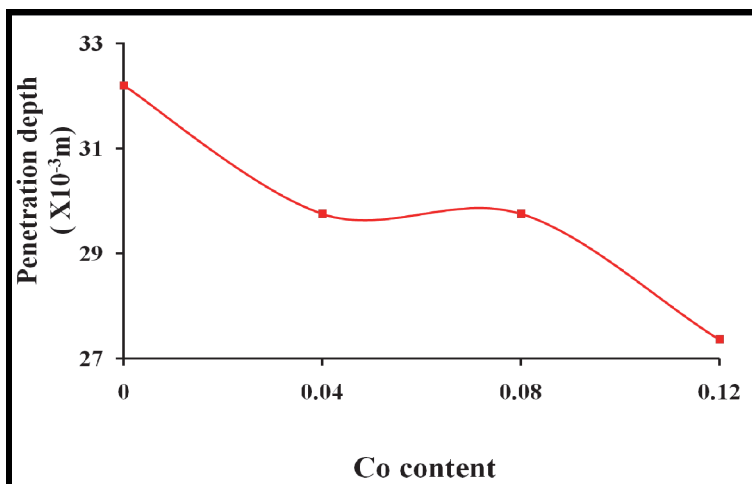


Fig. 6 – Dependence of penetration (microwave conductivity) depth on Co-concentration.

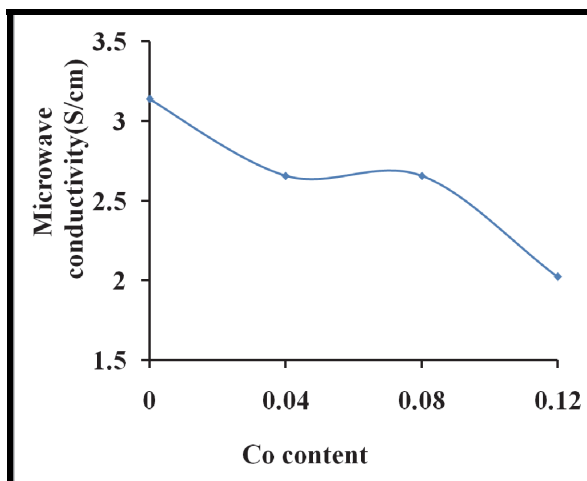


Fig. 7 – Dependence of microwave conductivity on Co-concentration.

The microwave conductivity was computed using the equation [13]

$$\sigma = \omega \varepsilon'' \varepsilon_0, \quad (7)$$

where  $\omega$  is angular frequency,  $\varepsilon_0$  and  $\varepsilon''$  are permittivity of free space and dielectric loss of material respectively.

The variation of microwave conductivity with cobalt (Co) content is shown in Fig. 7. It is observed that, the microwave conductivity decreases with the increase in cobalt content. The microwave conductivity lies in the range, of 2.02 S/cm-3.14 S/cm.

### 3 Conclusion

$\text{Ni}_{0.7-x}\text{Co}_x\text{Zn}_{0.3}\text{Fe}_2\text{O}_4$  thick films have been fabricated by cost effective simple technique of screen printing. The superstrate on Ag thick film MSRR is an efficient tool for detecting the cobalt composition-dependent changes in microwave properties of Ni-Zn ferrite thick films. The ferrite thick film superstrate on the MSRR results the resonance shifting to a lower frequency with a drastic improvement in the peak transmission. With the ring resonator set up the dispersion, dielectric constant, dielectric loss, penetration depth and microwave conductivity are measured. The dielectric parameters, penetration depth and microwave conductivity are found to vary with cobalt content. Thus superstrate technique was successfully implemented for the calculation of complex permittivity of the overlaid material and it is an efficient tool capable of detecting the changes in microwave properties. Hence these microstrip resonant circuits can be used as sensors to sense the moisture, extreme temperature, presence of gas etc.

### 4 Acknowledgment

Dr. S.N. Mathad is very much thankful to Prof. Gloria Albert, Head, Department of English, KLEIT, Hubli, India for precious English critique proofreading.

### 5 References

- [1] P. S. Anil Kumar, J. J. Shrotri, C. E. Deshpande, S. K. Date: Systematic Study of Magnetic Parameters of Ni-Zn Ferrite Synthesized by Soft Chemical Approaches, *Journal of Applied Physics*, Vol. 81, No. 8, 1997, pp. 4788 – 4790.
- [2] E. Rezlescu, L. Sachelarie, P. D. Popa, N. Rezlescu: Effect of Substitution of Divalent Ions on the Electrical and Magnetic Properties of Ni-Zn-Me Ferrites, *IEEE Transactions on Magnetics*, Vol. 36, No. 6, 2000, pp. 3962 – 3967.
- [3] A. Goldman: *Handbook of Modern Ferromagnetic Materials*, Springer Science+Business Media, LLC, New York, SAD, 1999.
- [4] A. C. F. M. Costa, V. J. Silva, D. R. Cornejo, M. R. Morelli, R. H. G. A. Kiminami, L. Gama: *Magnetic and Structural Properties of NiFe<sub>2</sub>O<sub>4</sub> Ferrite Nanopowder Doped with*

- Zn<sup>2+</sup>, *Journal of Magnetism Magnetic Materials*, Vol. 320, No. 14, July 2008, pp. e370 – e372.
- [5] S. B. Waje, M. Hashim, W. D. W. Yusoff, Z. Abbas: Sintering Temperature Dependence of Room Temperature Magnetic and Dielectric Properties of Co<sub>0.5</sub>Zn<sub>0.5</sub>Fe<sub>2</sub>O<sub>4</sub> Prepared Using Mechanically Alloyed Nanoparticles, *Journal of Magnetism Magnetic Materials*, Vol.322, No. 6, 2010, pp. 686 – 691.
- [6] T. Suzuki, T. Tanaka, K. Ikemizu: High Density Recording Capability for Advanced Particulate Media, *Journal of Magnetism Magnetic Materials*, Vol. 235, No. 1–3, 2001, pp. 159 – 164.
- [7] T. Giannakopoulou, L. Kompotiatis, A. Kontogeorgakos, G. Kordas: Microwave Behavior of Ferrites Prepared via Sol–Gel Method, *Journal of Magnetism Magnetic Materials*, Vol.246, No. 3, 2002, pp. 360 – 365.
- [8] M. George, S. S. Nair, A. M. John, P. A. Joy, M. R. Anantharaman: Structural, Magnetic and Electrical Properties of the Sol-Gel Prepared Li<sub>0.5</sub>Fe<sub>2.5</sub>O<sub>4</sub> Fine Particles, *Journal of Physics D: Applied Physics*, Vol. 39, No. 5, 2006, pp. 900 – 910.
- [9] A. B. Kulkarni, S. N. Mathad: Synthesis and Structural Analysis of Co-Zn-Cd Ferrite by Williamson-Hall and Size-Strain Plot Methods, *International Journal of Self – Propagating High-Temperature Synthesis*, Vol. 27, No. 1, 2018, pp. 37 – 43.
- [10] M. K. Rendale, S. D. Kulkarni, V. Puri: Microwave Dielectric and Attenuation Properties of Ni<sub>0.7-x</sub>CoxZn<sub>0.3</sub>Fe<sub>2</sub>O<sub>4</sub> Thick Films, *Microelectronics International*, Vol. 26, No.1, 2009, pp. 43 – 46.
- [11] R. N. Jadhav, V. Puri: Response of Ag Thick Film Microstrip Straight Resonator to Perturbation of Bulk and Thick Film Ni(1-x)CuxMn<sub>2</sub>O<sub>4</sub> (0≤x≤1) Ceramics, *Microelectronics International*, Vol. 28, No. 2, 2011, pp. 53 – 57.
- [12] S. N. Mathad, M. K. Rendale, R. N. Jadhav, V. Puri: Study of Lead Free Ferroelectrics Using Overlay Technique on Thick Film Microstrip Ring Resonator (MSRR), *Processing and Application of Ceramics*, Vol. 10, No. 1, 2016, pp. 41 – 46.
- [13] S. N. Mathad, R. N. Jadhav, R. P. Pawar, V. Puri: Dielectric Spectroscopy and Microwave Conductivity of Bismuth Strontium Manganites at High Frequencies, *Electronic Materials Letters*, Vol. 9, No. 1, 2013, pp. 87 – 93.